Energy 274 (2023) 127320

Contents lists available at ScienceDirect

Energy

journal homepage: www.elsevier.com/locate/energy

Complex study of bioplastics: Degradation in soil and characterization by FTIR-ATR and FTIR-TGA methods

R. Skvorčinskienė [a,*], I. Kiminaitė [a], L. Vorotinskienė [a], A. Jančauskas [a], R. Paulauskas [a]

[a] Laboratory of Combustion Processes, Lithuanian Energy Institute, Kaunas, LT-44403, Lithuania

ARTICLE INFO

Handling Editor: Petar Sabev Varbanov

Keywords:
Waste
Bioplastic
Pyrolysis
ATR-FTIR
TGA-FTIR

ABSTRACT

Today our society faces a twofold problem: the depletion of resources and the accumulation of waste. Today's market dictates that conventional plastics should be replaced by bioplastics, but there is a lack of research on using bioplastics, still sparking debates whether bioplastics are more sustainable than conventional plastics. This research investigates bioplastic degradation characteristics in soil (ATR-FTIR), thermal stability under pyrolysis and applicability for waste-to-energy using thermal analysis (TG) and evolved gas analysis (FTIR). Biodegradation experiments revealed that only bioplastic made of corn starch was able to completely and rapidly degrade in soil, while other bio-based and petroleum-based plastics only changed the colour and became softer. This proves that bioplastics are thermochemically altered and close in properties to conventional plastics, and solutions must be taken to recycle them properly or convert them into energy, otherwise, they are the exact source of microplastics. Thermogravimetric together with evolved gas analysis (TGA-FTIR) revealed that the gaseous yield from bioplastics is in the range of 80–99%, with the onset of degradation at 203.0–272.5 °C in N_2 environment, or 10–20 °C degrees below by enriching the environment with steam. Mainly, pyrolysis of volatile products of bioplastics are carboxylic compounds, alkanes, alkenes, aromatic hydrocarbons, amines, CO, and CO_2 depends significantly on the chemical composition of plastic.

1. Introduction

Over the last decades, the global plastic production has grown rapidly from 2 million metric tons (MT) in 1950 [1,2] to 367 million MT in 2020 (only in Europe – 55 million MT) [3]. At the moment, ~0.4 billion tons of plastic waste is generated, of which 12% are incinerated and about 9% are recycled [4]. As the rate of plastics production continues growing and consumerism is increasing, the amount of this waste will grow as well. In this context, there is a number of challenges around the world related to the non-sustainable and excessive use of plastics, microplastic pollution of the environment, and prominent carbon footprints. Every year the production and incineration of plastics release around 400 million tons of carbon dioxide into the atmosphere [5]. Some of this could be avoided by achieving the targets of Green Deal which promotes the growth of Green Energy and environmentally sustainable products [6], as well as highlight the transition to a circular economy [5]. The United Nations Development Programme (UNDP) is aimed to achieve sustainable economy, efficient use of natural resources, and reduced pollution in the face of growing environmental and climate control challenges. All trends point to a global drive towards sustainable economy through efficient use of renewable natural resources and reducing pollution and waste generation [7,8]. It is believed that one way to reach energy sustainability is to produce biodegradable or bio-based polymer materials, also known as bioplastics [9]. The bioplastics [10] can be biodegradable or thermochemically degradable (bio-based) substances that have similar properties to conventional polymer materials, as well as it can be easier to recycle and degraded faster than plastic, thus contributing to sustainability. These bioplastics can be biodegradable or non-biodegradable and are made from bio-based products derived from plants and other renewable agricultural and/or petroleum products. Fossil-based biodegradable plastics include the polycaprolactone (PCL) [10], polyvinyl alcohol (PVA) [11], polybutylene adipate terephthalate (PBAT) [11] and polyvinyl alcohol copolymers, with the addition of a certain amount of ethylene in the composition of these alcohol copolymers (EVOH) [12]. The bio-based non-biodegradable bioplastics are polyamides (bio-PP), polyethylene terephthalate (bio-PET), polyethylene (bio-PE) [13], as well as bio-polytrimethylene terephthalate (bio-PTT), and bio-polyamide

* Corresponding author.
E-mail address: Raminta.Skvorcinskiene@lei.lt (R. Skvorčinskienė).

https://doi.org/10.1016/j.energy.2023.127320
Received 30 October 2022; Received in revised form 22 March 2023; Accepted 23 March 2023
Available online 2 April 2023

(bio-PA) [14].

The production of bioplastics usually starts from biomass undergoing a series of modifications like pre-treatment and hydrolysis, and then fermentation is carried out to produce bioethanol [14]. Then, the bioethanol is converted to non-biodegradable bioplastics. Bio-based biodegradable bioplastics are polylactic acid (PLA) [15], polyhydroxyalkanoates (PHAs) [16] and bio-based polybutylene succinate (bio-PBS) [17], also plastics based on cellulose, lignin, chitosan and starch [18]. Despite established stereotypes, as an example, polybutylene succinate (PBS) can also be made from both bio-based feedstock and petroleum [19]. European Bioplastics has published a market analysis estimating global bioplastics production at around 2 MT in 2018 [20]. In Europe, the consumption of plastic waste from biodegradable materials has been increasing [21], for example, the production of bioplastics increased by around 11% between 2015 and 2019. Bioplastics production was expected to increase by no less than 40% by 2025 [22], but the growth is now projected to be less rapid. These numbers show that the bioplastics as a product are not yet completely ready for the market. Therefore, recent research is aimed at improving the properties of bioplastics such as hardness, brittleness, thermal stability and stiffness [22]. About half of the current bioplastic materials are non-biodegradable, which will make it difficult to allocate it end-of-life as production increases [14]. Without proper life cycle management of bioplastics, the situation can become unmanageable, causing great concern [23]. These aspects do not allow to trust the quality of bioplastics after end-of-life and raise doubts about physical properties of products. Some products claimed to be biodegradable may degrade in the natural environment, but the study [24] has shown that products do not degrade within a specified period of time due to numerous modifications and require the bioreactions and specific conditions. Generally, conventional plastic is not environmentally friendly due to low recycling rate [25] and guaranteed source of microplastics [26]. In terms of waste-to-energy methods, pyrolysis can be highlighted as an efficient method due to material compatibility. During the pyrolysis [27] of bioplastics, it is possible to obtain gaseous products that would serve as a substitute for fossil fuels in meeting the aspects of renewable energy sources [28]. In addition, higher value-added products can be obtained [29].

According to scientific literature, bio-based bioplastics which are biodegradable and can degrade within 6 months are viewed controversially and additional studies are required. For these reasons, this study aimed to highlight the disadvantage of bioplastics in order to offer a solution for its utilization way. This study focuses on complex investigation of short-term (up to six months) biodegradation characteristics and pyrolysis options of various samples by using methods of attenuated total reflectance infrared spectroscopy analysis (ATR-FTIR), thermogravimetric analysis (TG) and evolved gas analysis (FTIR). In addition, evaluation of thermal stability of bioplastics belonging to different groups was performed to determine suitable utilization methods and it also plays an important role for future efforts to use bioplastics for waste-to-energy (gas) conversion.

2. Materials and methods

The coming future market dictates that bio-based bioplastics must increase significantly and replace the market of conventional plastic. It is stated that plastic waste issues can only be addressed by developing bio-based bioplastics that avoid do not contain petroleum-based degradable materials. However, more research is focusing on the problem of creating the specific conditions needed for bioplastics to start degrading. It has also been observed that modifications to the raw materials, such as hydrolysis, change the properties of the material and make bio-based bioplastic a source of micro-nano plastics. Pyrolysis was carried out immediately when the results obtained on the non-degradability of bioplastics were confirmed. The influence of steam on thermal degradation was also investigated in order to have a more effective conversion process. Twelve different (bio)plastics samples were chosen for this study. The principal scheme of the study covering all the procedures performed in the study is presented in Fig. 1.

2.1. Used materials

The analysis of 12 different samples used in the beauty, hygiene and packaging fields (see Fig. 2 has been carried out. All samples were divided into four groups (from A to D) regarding to bioplastic/plastic nature by colour. The samples in the group A (light green) represents bioplastics which are bio-based but non-biodegradable (TB1, SCP, TB3), the samples in group B (in green) are bio-based and biodegradable (TP, CGB, FO, SPLA, SPP). The group C consists of a petroleum-based bioplastic (PWB), which is supplemented with some materials needed for degradation, and presented in dark blue. The group D consists of remaining samples (light blue) made of petroleum-based plastics (TB2, TH1, TH2) which are recyclable. The concluded groups of all samples are presented in Fig. 3.

To fully define selected plastic materials, the ultimate and proximate analysis of plastics was carried out using an IKA C5000 calorimeter and a Flash 2000 CHNS analyser according to the standards: ISO 15512:2019 – the water content [30]; ISO 21654:2021 – the higher heating value [31], ISO 21656:2021 the ash content [32], ISO 22167:2021– the volatile content [33] and ISO 21663:2020 – the CHNS content [34]. The obtained characteristics are presented in Table 1.

2.2. Setup and procedure for plastic biodegradation under real conditions

The experiment of plastics biodegradation was performed under real conditions and lasted for 6 months. For the experiment, the open field and remote location (the territory of the Lithuanian Energy Institute, Kaunas, Lithuania), away from heavy traffic and buildings were chosen. These conditions ensured that the experimental setup receives a representative amount of the precipitation and sun radiation. To investigate the biodegradation of selected plastics, a pit of rectangle form with dimensions of LxWxD – 116 × 76 × 40 cm was dug. A wooden frame was inserted in the bottom of the pit and three quarters of this box volume was filled with a blend of cattle manure, peat, and wood shavings (see Fig. 4).

This blend was prepared based on Kale et al. [35] research: 28% of cattle manure and 72% of compost. According to information provided by distributors, the manure was supplied without pathogens, and did not contain any weed seeds. The formed layer of the compost was divided into 12 rectangles (25 × 28 cm) using stainless steel strips and each rectangle was filled with different samples (Fig. 4). Bags, bottles and bag films were additionally prepared for biodegradation tests under natural conditions by cutting them into small pieces to ensure uniform exposure to oxygen and bacteria. The samples were placed at the centre of the corresponding area and covered with the compost. Scheme of the arrangement of samples is shown in Fig. 4. For easier inspection, the box of samples was covered with the stainless-steel mesh and the top was filled with soil, sourced from the same area and covered with lawn grass. Soil temperature changes were measured at the middle of the box cross-section and at the level of test samples (Fig. 4). The temperature inside and outside the box was registered by an OMEGA RDXL6SD data logger connected with 4 K-type thermocouples, i.e., TS_1-TS_4. Each thermocouple was coated with a hydro-insulation for protection of corrosive environment and to ensure precise measurements. Temperature readings from thermocouples were cross-checked with water boiling point. The data logger was placed underground in a hermetically sealed box near the sample box for continuous temperature monitoring. Set periodicity of the temperature measurement – 1 h. The acidity (pH) and relative moisture content (0–10) of the soil were measured with a portable meter TAC002. The soil pH and moisture content were measured at the corner (SS_1) of the box in order to avoid any harm for samples by penetrating the soil with the probes (Fig. 4). The average soil

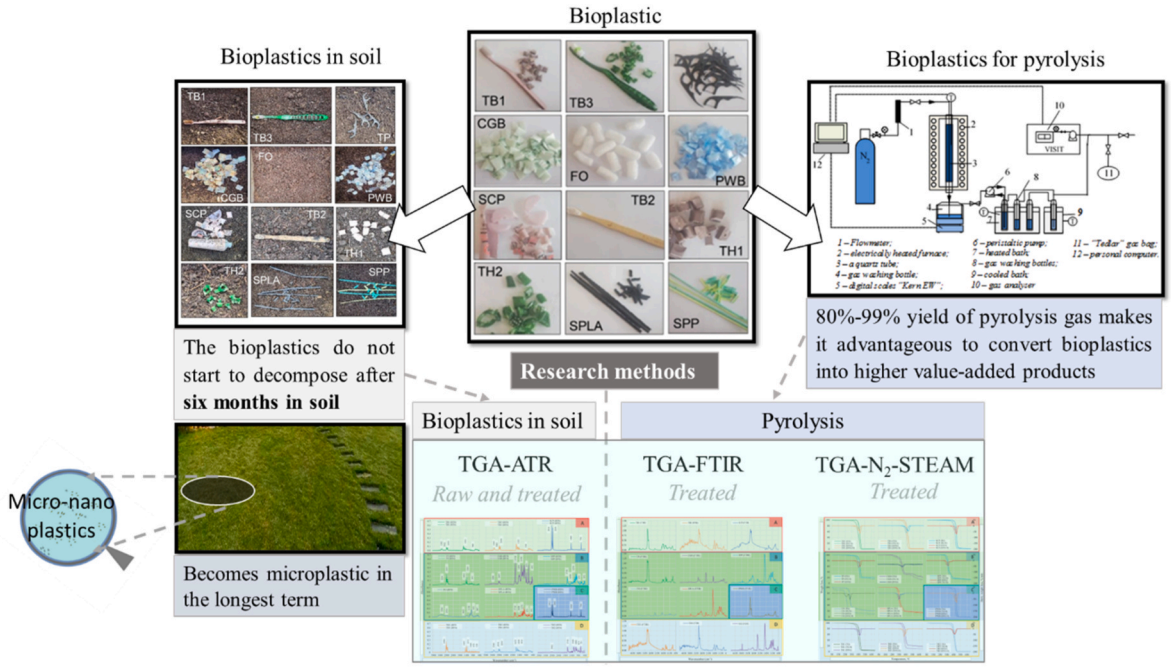

Fig. 1. The principal scheme of the research.

pH moisture content during the entire period (6 months) varied from 6.3 to 7.0. Also, the parameters of local air temperature and relative humidity were collected during all experimental period according to real-time weather observations in "Meteociel" database, where historical meteorological condition of Kaunas is registered and publicly available. The experiments started at June 10, 2022 and lasted for six months.

2.2.1. Fourier-transform infrared analysis of plastic samples

The bonds and functional groups in the raw and treated bioplastics samples were identified using Bruker Tensor 27 IR spectroscope using the attenuated total reflectance Fourier transform infrared spectroscopy (ATR-FTIR) analysis recording the spectra in the 4000-650 cm^{-1} wavenumber range and the obtained data are presented in the following sections. The scan resolution in FTIR was set at 4 cm^{-1} and the sample scan time - 32 s. The IR Analyze software was used for the advanced infrared spectrum identification and interpretation.

2.3. Pyrolysis and thermal analysis

Thermogravimetric analysis of plastic wastes was performed using NETZSCH STA 449 F3 Jupiter analyser with a SiC furnace in accordance of a standard method ASTM E2550. The DSC sample carrier with the S-type thermocouple was calibrated for 200 mg Al_2O_3 TG crucibles. In this study, the samples in 5–10 mg amounts were placed in the Al_2O_3 crucible in the TGA chamber along with a reference crucible, and the sample was heated at 20 °C/min ramp steps up to 700 °C. The nitrogen gas flow rate of 60 ml/min was used to maintain an inert atmosphere in the furnace to perform pyrolysis and to evaluate the main thermal events occurring during this thermochemical conversion process.

In order to evaluate the behaviour of selected plastics under gasification conditions, TGA was also performed in a partially oxidising environment by supplying nitrogen gas along with steam. The process temperature and heating rate were set equal to those applied previously during pyrolysis experiments, except the process atmosphere was supplemented with steam. The flow of streams supplied to the furnace was set as following: nitrogen as a protective gas was fed at 60 ml/min rate and steam (relative humidity of 60%) at 60 ml/min, employing pure nitrogen gas as a dry flow. Obtained thermogravimetric curves in both analysis cases were used for thermal stability determination of selected plastic materials according to the weight loss at defined temperature points.

2.3.1. FTIR analysis of volatile pyrolysis products

Volatile compounds evolved during pyrolysis of each sample at their main decomposition temperatures (according to the DTG curves) were simultaneously analysed by means of Fourier-transform infrared spectroscopy (FTIR) by measuring absorption of IR rays in the wavenumber range of 4500–650 cm^{-1}. Gases formed during thermal decomposition of plastic samples were collected through the transfer line to the FTIR gas cell. Both transfer line and gas cell were heated to prevent condensation of volatile compounds of higher molecular mass. Mercury cadmium telluride (MCT) detector that operates at the liquid nitrogen temperature was used for the registration of IR absorption. Gas composition was analysed with FTIR during all the experiments of each sample every 14 s performing scans at 4 cm^{-1} resolution.

3. Results and discussion

3.1. The biodegradability test of bioplastic in soil

During the six months of biodegradability (BT) experiment, the soil ambient temperature and precipitation data were collected (see Fig. 5). The average compost temperature is derived from the hourly average of thermocouple temperatures TS_2 and TS_3 (see Fig. 4), and the temperature of surrounding soil from the TS_1 and TS_4 thermocouples. At the beginning of the experiment, initial compost and soil temperatures were higher compared with the next week temperature average. This is due to preparatory works when the excavated compost and soil were temporarily exposed to a higher ambient temperature and solar radiation. After the experimental equipment was set up, a temperature inside the composter was significantly higher. For example, on July 10, the average temperature inside the composter was 26.3 °C and up to 2.0 °C higher than the surrounding soil. A higher temperature inside the compost was also measured by G. Kale et al. [35]. These temperature differences decrease along with the average temperature. On the last day of measurements, i.e., on December 10, the average temperature inside the composter decreased to 5.2 °C and was 0.2 °C degrees lower

No.	Product	Volume of recycled plastic	Type of plastic	Marking	Petroleum based plastic	Bio-based bioplastic	Biodegradable	Compostable	Recyclable	Properties	Labeling
TB1	Toothbrush bristles No. 1	0%	Bioplastic naylon-polyamide	PA	0%	100% bio-based nylon, originating from castor oil plants	NO	NO	YES	Transparent, flexible, hard	
SCP	Sugarcane bioplastic bottle	0%	Bioplastic / polyethylene	Bio-based PE + petroleum based PE	47% PE	Sugarcane 53%	NO	NO	YES	Greyish brown, not transparent, hard, flexible	
TB3	Toothbrush bristles No. 3	0%	Bioplastic naylon-polyamide	PA	2%	98% originating from castor oil plants	NO	NO	YES	Flexible, white	A
TP	Dental floss holder (toothpick)	0%	Corn Starch / Polypropylene	PP+ corn	30% PP	70% corn starch	Partially	NO	YES	Black, slightly brittle, hard, flexible	
CGB	Compostable garden bags	0%	Corn Starch	-	0%	100% corn starch	YES	YES	NO	Green, transparent	
FO	Biodegradable packing foam	0%	Corn Starch	-	0%	100% corn starch	YES	YES	NO	White, light, flexible, porous	
SPLA	Flexible Straws	0%	Biological origin	PLA	0%	100%	YES	YES	NO	Flexible, not transparent, green	
SPP	Flexible Straws	0%	Biological origin	PLA	0%	100%	YES	YES	NO	Flexible, not transparent, black	B
PWB	Pet waste bags	0%	Polyethylene / Reverte	HDPE+Reverte	100%+ REVERTE	0%	YES	NO	YES	Elastic, colored (blue, rosy)	C
TB2	Toothbrush bristles No. 2	0%	NAYLON - polyamide	PA	100%	0%	NO	NO	YES	White, elastic, hard, resistant to abrasion,	
TH1	Toothbrush handle	100%	Polyethylene terephthalate	RPET	100%	0%	NO	NO	YES	Greyish-brown, not transparent, hard	
TH2	Toothbrush handle	100%	Polyethylene terephthalate	RPET	100%	0%	NO	NO	YES	Green, not transparent, hard	D

Fig. 2. Characteristics of the bioplastics.

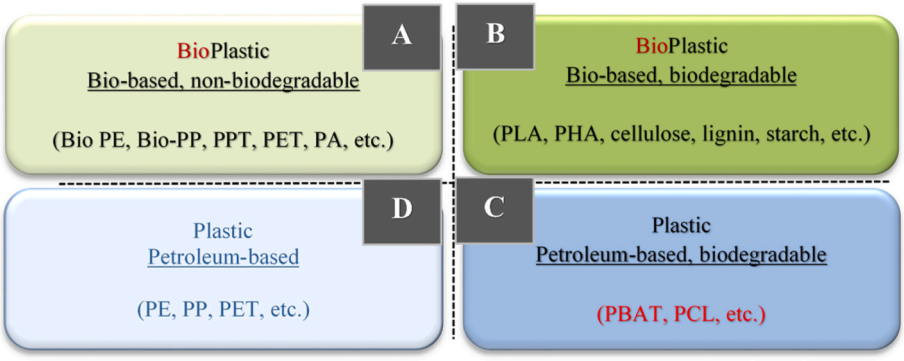

Fig. 3. Types of bioplastics.

Table 1
Proximate and ultimate analysis results of the selected samples.

Sample	Ultimate analysis (wt.%)					Proximate analysis (wt.%)			
	C	H	N	S	O	Moisture	Volatile Matter	Fixed Carbon	Ash
TB1	70.69	11.38	8.68	<0.01	9.25	0.40	99.60	0.00	0.00
SCP	83.83	14.14	<0.01	<0.01	0.58	0.21	98.34	0.07	1.45
TB3	69.68	11.21	8.83	<0.01	9.89	0.65	98.97	0.26	0.38
TP	69.93	11.63	<0.01	<0.01	5.45	0.10	86.03	0.89	12.98
CGB	50.22	5.34	<0.01	<0.01	31.00	0.25	82.02	4.29	13.44
FO	41.90	6.64	<0.01	<0.01	45.34	3.33	76.43	14.11	6.13
SPLA	47.37	5.23	<0.01	<0.01	36.04	0.25	86.00	2.39	11.36
SPP	47.15	5.24	<0.01	<0.01	36.17	0.12	86.78	1.66	11.44
PWB	85.06	14.55	<0.01	<0.01	0.28	0.22	99.67	0.00	0.11
TB2	69.15	11.05	9.56	<0.01	8.83	0.59	98.00	0.25	1.41
TH1	84.28	14.19	<0.01	<0.01	0.00	0.27	97.98	0.19	1.75
TH2	62.62	4.29	0.11	<0.01	32.27	0.10	83.43	15.77	0.70

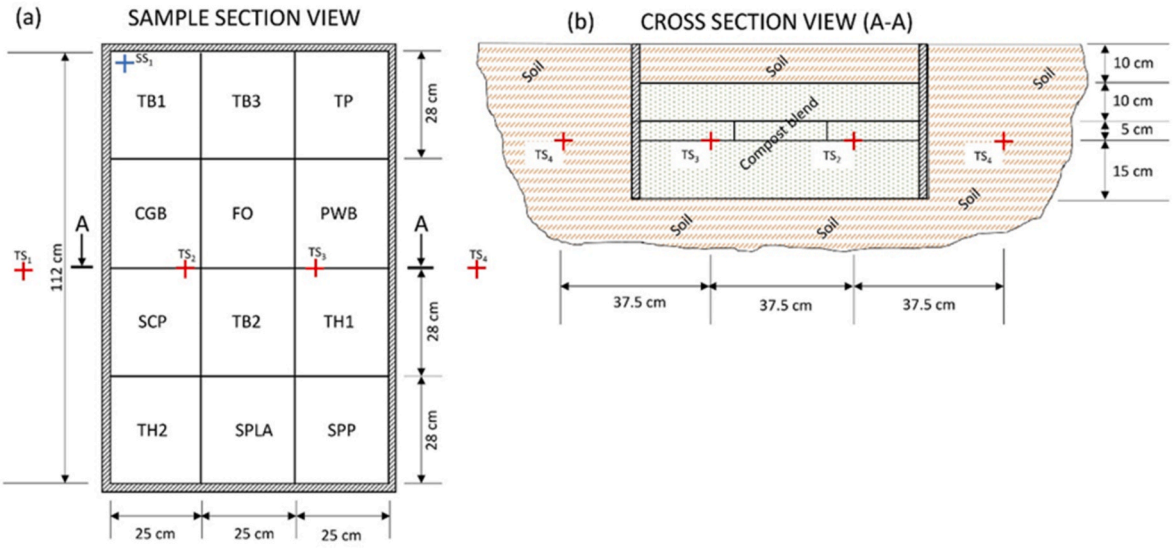

Fig. 4. Experimental compost blend box (a) and on-site view (b).

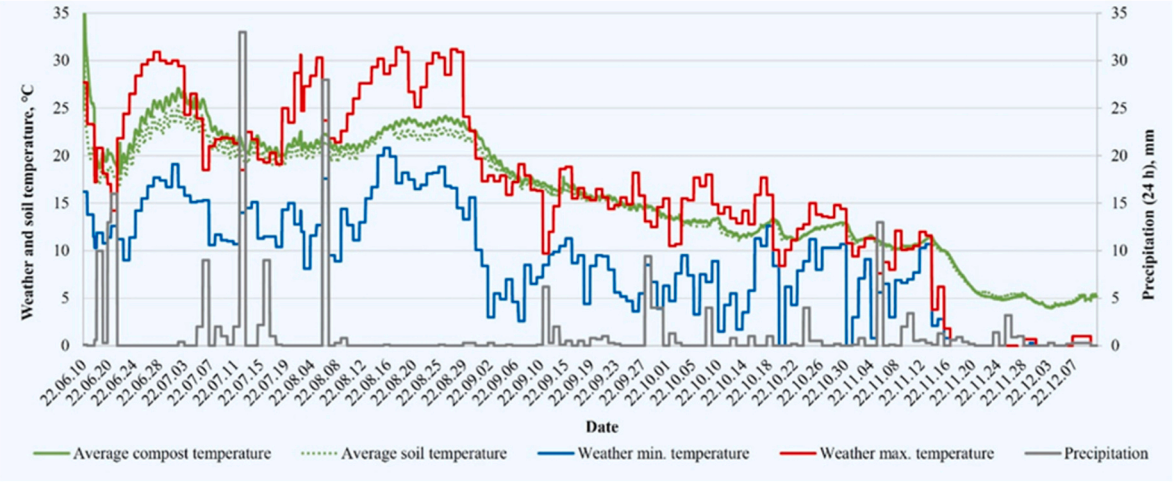

Fig. 5. Research conditions of biodegradability of plastics.

compared with the surrounding soil. Moreover, changes of short-term climatic conditions such as the weather temperature and precipitation have a significant impact on the compost and surrounding soil temperatures, as can be seen at rainy periods in 15–22 of June, 4–18 of July and 5–10 of August. It was also noticed that the compost and soil temperatures are characterized by fluctuations that have appeared as a result of daytime and nighttime temperature differences. On July 10, the temperature difference between the compost minimum and maximum temperature was 2.5 °C. On July 10, the maximum and minimum temperature difference was 1.4 °C, while on December 10 it was only 0.1 °C.

In order to determine the effect of bioplastic biodegradability in the soil within 6 months period, ATR-FTIR analysis of raw (prior to biodegradation – BT0) and treated samples (after biodegradation – BT6) was performed. The obtained data was divided into groups based on Fig. 3 and the non-biodegradable bioplastic group consisting of TB1, TB3 and SCP was analysed in the first place. A visual inspection of these samples has not shown any signs of biodegradation, though colour of TB1 and TB3 has changed a bit (see Fig. 6).

The manufacturer of the TB1 and TB3 products (group A) states that these bioplastics are made from bio-based nylon (respectively 100% and 98% of TB1 and TB3). The ATR-FTIR analysis confirmed that the main component of TB1 and TB3 is nylon (see Fig. 7 A), although the spectrum of bio-based material is closely similar to one of fossil-based polyamide fibers. During FTIR analysis it was found that the peaks at absorbance bands of 3303 cm^{-1} and 3082-3080 cm^{-1} indicate secondary amine N–H vibrational range and polymer chain CH asymmetric valence aliphatic vibrations, respectively [36]. In the band range from 2920 to 2850 cm^{-1}, the determined peaks indicate existence of methylene C–H stretch groups, while peaks at absorbance bands of 1535 cm^{-1} and 1635 cm^{-1} correspond to amide group NH bending and carbonyl C═O vibrations, respectively [37]. In the range from 1456 to 1380 cm^{-1} and from 1470 to 1380 cm^{-1} are observed C–H bend and CH_2/CH_3 respectively for TB1 and TB3. Moreover, the peaks at 937 and 940 cm^{-1} correspond to C–CO group. A different composition was determined analysing the SCP sample (group A). According to ATR-FTIR spectra, three spectral groups were determined which correspond to the polyethylene group. Peaks at absorbance bands of 2914 cm^{-1}, 2850 cm^{-1}, 1460 cm^{-1} and 720 cm^{-1} could be attributed to methylene group ranges of CH_2 asymmetrical stretch, $–CH_2-$ symmetrical stretch, $–CH_3$ umbrella mode and $–CH_2-$ rocking peak [36], respectively (Fig. 7 A). However, ATR-FTIR analysis of treated samples indicated the same absorbance peaks and there were no changes in structure of this group bioplastics during biodegradability tests.

The second group (group B) was bio-based biodegradable bioplastics and according to an inspection after 6-month degradation in the soil, TP, CGB, SPP, FO, SPLA underwent more prominent changes in color and strength. Additionally, the sample FO has fully degraded. The group B samples were made from 100% corn starch which resulted in the full decomposition in moist environment. A similar trend was observed with sample TP which also consists of corn starch. The sample has lost solidity, become soft, albeit the color has not changed a lot. SPLA and SPP samples lost color and changes in ductility were observed – samples became rigid. Meanwhile, the CGB sample – a bag which is designed for composting biodegradable wastes, has only lost color and visual surface changes were observed after biodegradation experiments (Fig. 6). The ATR-FTIR analysis confirmed that the composition of TP sample which contains 30% of corn starch as peaks at specific bands described below corresponds to polypropylene and a wide peak at the band of 3258 cm^{-1} indicates OH group [38] (Fig. 7 B).

Vibrations in the band range from 2957 to 2836 cm^{-1} are due to aliphatic C–H asymmetrical and symmetrical stretching, while determined vibrations at 1454 cm^{-1} and 1369 cm^{-1} wavelengths respectively are CH_3 asymmetrical and symmetrical deformations [38]. Also, a negligible peak is observed at 1163 cm^{-1} wavelength, caused by C–C asymmetric stretching, while in the range of 997–972 cm^{-1} occurred scissors bend due to CH_3 asymmetrical vibration [38]. Meanwhile, peaks in band range of 710–509 cm^{-1} wavelength occurred due to impurities indicating C–H aromatic compounds [39].

The ATR-FTIR analysis allowed determination of the functional groups of the CGB, SPP and SPLA samples (group B), which contributed to the identification of the product's main component as polylactic acid (PLA). According to the obtained spectra of CGB, SPP and SPLA samples, the peaks at bands of 2956–2875 cm^{-1}, 2996-2850 cm^{-1} and 297-2852 cm^{-1} are present due to the asymmetrical and symmetrical C–H vibrations origination in polymer comprising molecules [40] (Fig. 7 B). At wavelength bands of 1710, 1748 and 1748 cm^{-1}, the determined peak could be present due to stretching vibration of carbonyl group C═O [40]. Also, absorbance spectra of CGB, SPP and SPLA samples indicate a small peak at 1450 cm^{-1} wavelength, which is possibly caused by CH_3 symmetrical deformation vibration, while CH deformation vibration was obtained at 1270 cm^{-1}, 1268 cm^{-1} and 1267 cm^{-1} wavelengths [41] respectively for CGB, SPLA and SPP. More intense group of peaks in spectra of CGB, SPLA and SPP was observed respectively in the band range of 1099–1014 cm^{-1}, 1084-1014 cm^{-1} and 1082-1012 cm^{-1} wavelengths and these could be related to $C–CH_3$ functional group stretching vibration, while in range of 728–664 cm^{-1}, 729-668 cm^{-1} and 728-664 cm^{-1} C═O stretching vibration peak [41] is present. The peaks at 875 cm^{-1}, 868 cm^{-1} and 870 cm^{-1} correspond to the C–O bending and stretching vibration that are specific for $CaCO_3$ [42]. Thus, it was indicated that some amount of $CaCO_3$ was present in CGB, SPLA

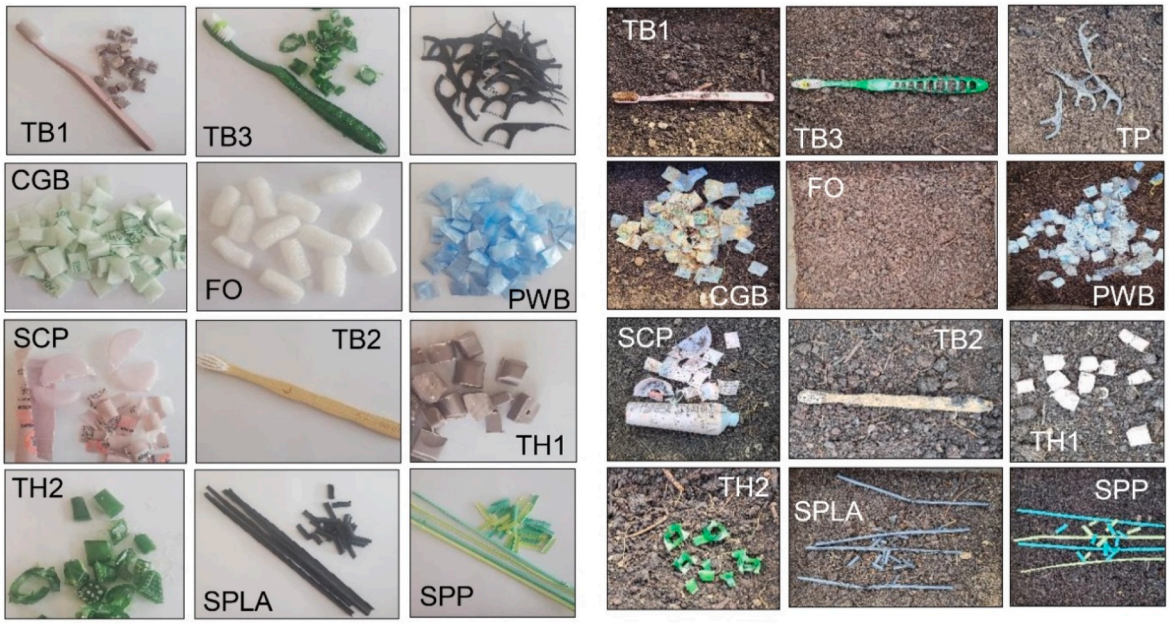

Fig. 6. Images of plastics before (left – BT0) and after (right – BT6) biodegradability tests.

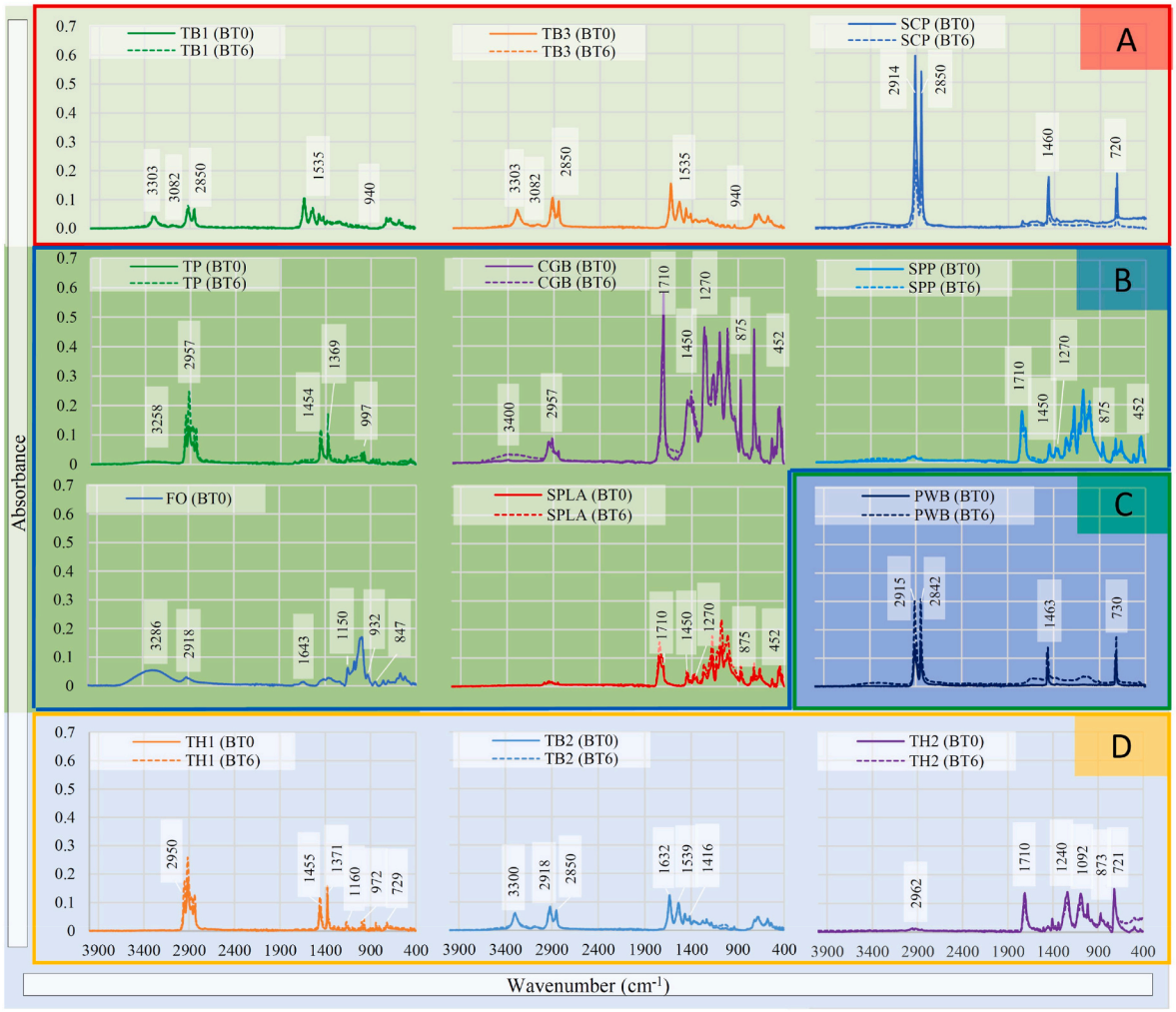

Fig. 7. ATR-FTIR spectra of raw (BT0) and treated (BT6) samples.

and SPP bioplastic samples, since it provides higher tensile strength to bioplastic materials [43]. Analysing the fingerprint zone, small peaks were determined at bands of 452, 447, 445 cm^{-1} due to C–CO vibrations [44]. After biodegradation experiments of these samples, only valence vibrations of OH group were determined at 3400, 3300, 3341 cm^{-1} wavelengths indicating inception of ongoing biodegradation due to interactions with environment (Fig. 7 B). The ATR-FTIR analysis of the FO sample shows a band peak of OH valence vibrations at the band of 3286 cm^{-1} wavelength, which is attributed to a polysaccharide group, and a small peak at 2918 cm^{-1} due to aliphatic vibrations of C–H groups. At the band of 1643 cm^{-1} wavelength, a small wide OH peak was observed indicating presence of moisture in the sample. In the range of 1150–1014 cm^{-1} were determined peaks related to C–C and C–O vibrations. Also, small peaks possible due to vibrations of C–O alkanes were observed in the band range of 1414–1368 cm^{-1}. Considering that the accurate composition of the FO samples is not known, observed peaks in the fingerprint zone at the band of 932 cm^{-1} might be related to vibrations of C_2H_4 alkanes. At the band of 847 cm^{-1}, a small formed peak could be considered as an indication of aromatic hydrocarbonates, but evaluating negligible peaks in the fingerprint zone is challenging and there is no clear peak at 3000 cm^{-1} indicating aromatic group presence (Fig. 7 B).

The sample of the group C is the biodegradable petroleum-based plastic. After the biodegradability experiments, the sample has lost color and shrunk (Fig. 6). This material is made on the basis of polyethylene with impurities accelerating the degradation of plastic, but the amount of impurities is very low according to the ATR-FTIR analysis, as only 3 main groups were determined (Fig. 7 C). In the range of 2915–2842 cm^{-1}, an aliphatic valence peak is present due to C–H asymmetrical and symmetrical stretching [45]. The second peak at 1463 cm^{-1} is formed due to polyethylene CH_3 umbrella bending mode and the third one is present due to CH_2 rocking vibration at the band of 730 cm^{-1}.

The inspection of non-biodegradable petroleum-based plastics indicates that only negligible changes in color of TB2 and TH1 have occurred after 6-month presence in the soil (Fig. 6). The ATR-FTIR analysis shows that the sample of TH1 is made on basis of polypropylene and the spectra is close to one of TP, which is attributed to the group of bio-based and biodegradable plastics. The intense range of four peaks in the band range of 2950–2836 cm^{-1} is attributed to the C–H asymmetrical and symmetrical stretching [46] (Fig. 7 D). The peaks caused by CH_3 asymmetric and symmetric deformation vibrations were determined at bands of 1455 cm^{-1} and 1371 cm^{-1} respectively [47]. Also, TH1 spectra shows small peaks at 1160 and 972 cm^{-1} wavelengths possibly formed due to C–C asymmetrical stretching and in the range of 992–972 cm^{-1} due to CH_3 asymmetric oscillating vibrations [47]. In the range of 729–509 cm^{-1} peaks are might due to C–H aromatic group occurred from impurities of petroleum compounds [47]. FTIR analysis of TB2 sample shows a bit different sample composition. At band of 3300 cm^{-1} peak is due to N–H bonds and scissor peak in the range of 2918–2850 cm^{-1} could be related to C–H stretch vibrations [37]. Also, N–H peak at 1539 cm^{-1} is attributed to secondary amine due to primary

amine conversion. At the band 1632 cm^{-1} an intensive peak of N–H indicates amides group. In the range of 1467–1416 cm^{-1} small scissor peak could be present due to C–H bending vibrations [38]. FTIR spectra of TH2 sample reveals groups of peaks related to RPET functional groups. At the band of 2962 cm^{-1} observed small peaks could be present due to C–H group vibrations. An intense peak determined at bands of 1710 and 1092 cm^{-1} shows C═O aldehyde vibrations and at 1240 cm^{-1} the observed peak is due to C–O vibrations. Intense peaks at 873 and 721 cm^{-1} wavelengths are present due to C–H [48] (Fig. 7 D).

The performed FTIR analysis indicates that the biodegradation changes of the bioplastic did not occur within 6 months. Due to these reasons, further section of this study focuses on thermal decomposition of these bioplastics to recover valuable products and produce energy.

3.2. TGA-DTG analysis

In order to evaluate thermal stability of selected plastic materials, experiments of thermogravimetry (TGA) combined with differential thermogravimetry (DTG) were carried out. Obtained curves are presented in Fig. 8. Main thermal decomposition points of bioplastics were identified based on the obtained TGA-DTG results. Onset temperatures of thermal decomposition (that also describe thermal stability of material) were determined from TGA curves, whereas the peaks in DTG curves revealed at which temperatures the mass loss rates reached maximum values during the thermal decomposition in inert versus steam environment. Described temperature points of four analysed groups of bioplastics are displayed in Fig. 9. It was evaluated, that onset temperatures (Onset TG) of thermal degradation in the inert atmosphere were either higher or close to the ones estimated in steam atmosphere (Onset TG-S) in all cases. DTG peak (DTG, DTG-S) temperatures were likewise determined to be higher in the N_2 atmosphere (Figs. 8 and 9). This tendency is explained by the hydrolysis effect of steam supplied to the furnace that intensified thermal degradation [49], consequently reducing the temperature of decomposition onset point. Additionally, it was estimated that steam supply to the furnace during pyrolysis promoted the decomposition of samples, since a higher proportion of volatile compounds were formed compared to the pyrolysis in N_2 atmosphere. TGA of plastic samples have revealed that analysed polymers decompose mainly into volatile matter forming a minor part of char with an exception of bio-based and biodegradable plastics that were determined to have higher contents of fixed carbon (Table 1). The highest formation of volatiles during the thermal decomposition was determined for conventional plastic wastes attributed to groups C and D, as well as bio-based non-biodegradable plastics (group A) (see Fig. 8).

The obtained TGA graphs (Fig. 8) have revealed that non-biodegradable samples made of biological origin materials (bioplastics attributed to group A) and conventional plastics (groups C&D) have decomposed in single degradation stage at both inert and steam atmosphere that suggest that particular samples are primarily made of one polymer or couple of polymers that belong to the same type. Whereas this characteristic of decomposition in one stage was observed in only one sample of bio-based and biodegradable plastics (group B), namely

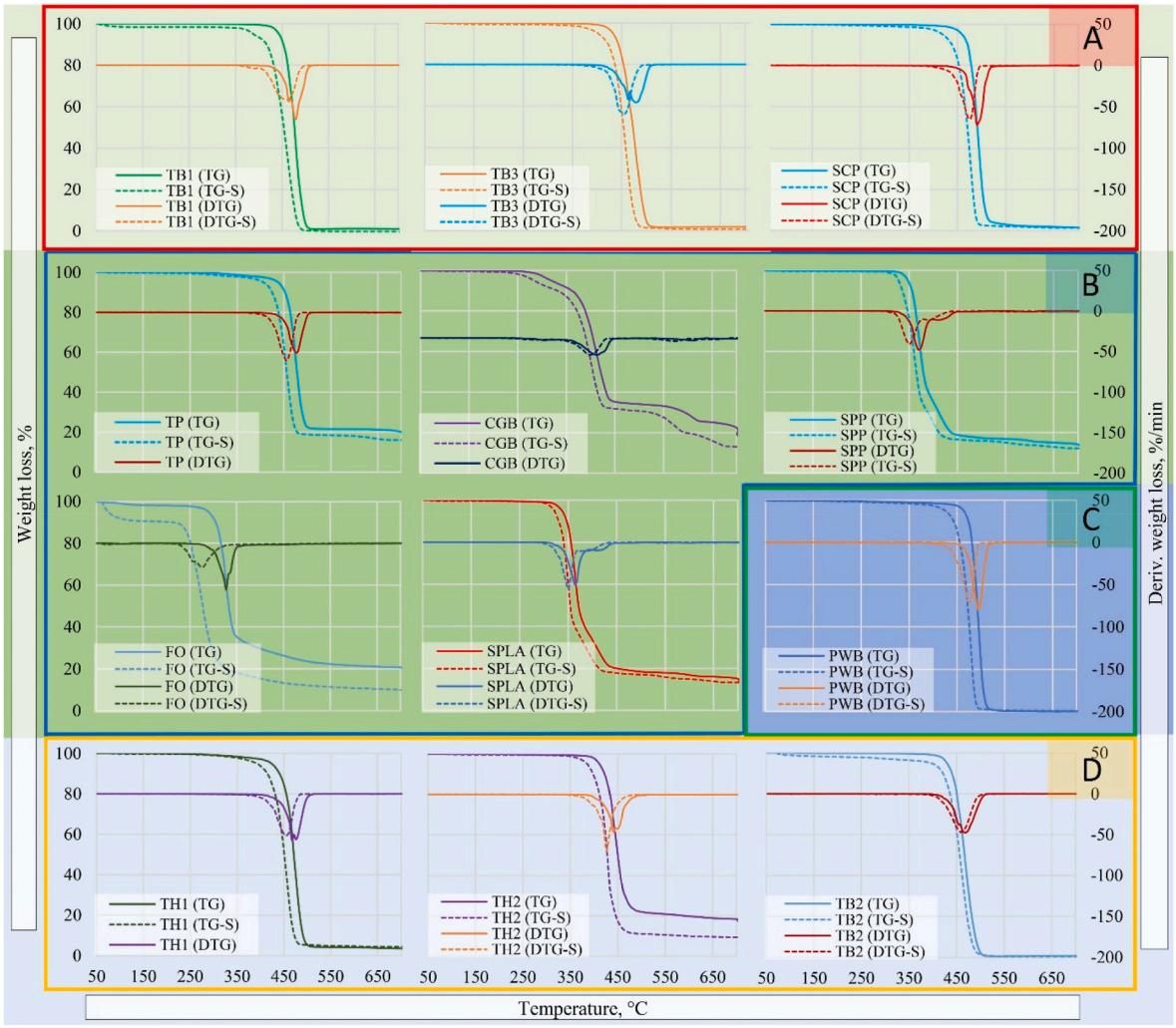

Fig. 8. TGA-DTG curves of plastic samples obtained in inert environment of N_2 (TG, DTG) and partially oxidising environment of steam (TG-S, DTG-S).

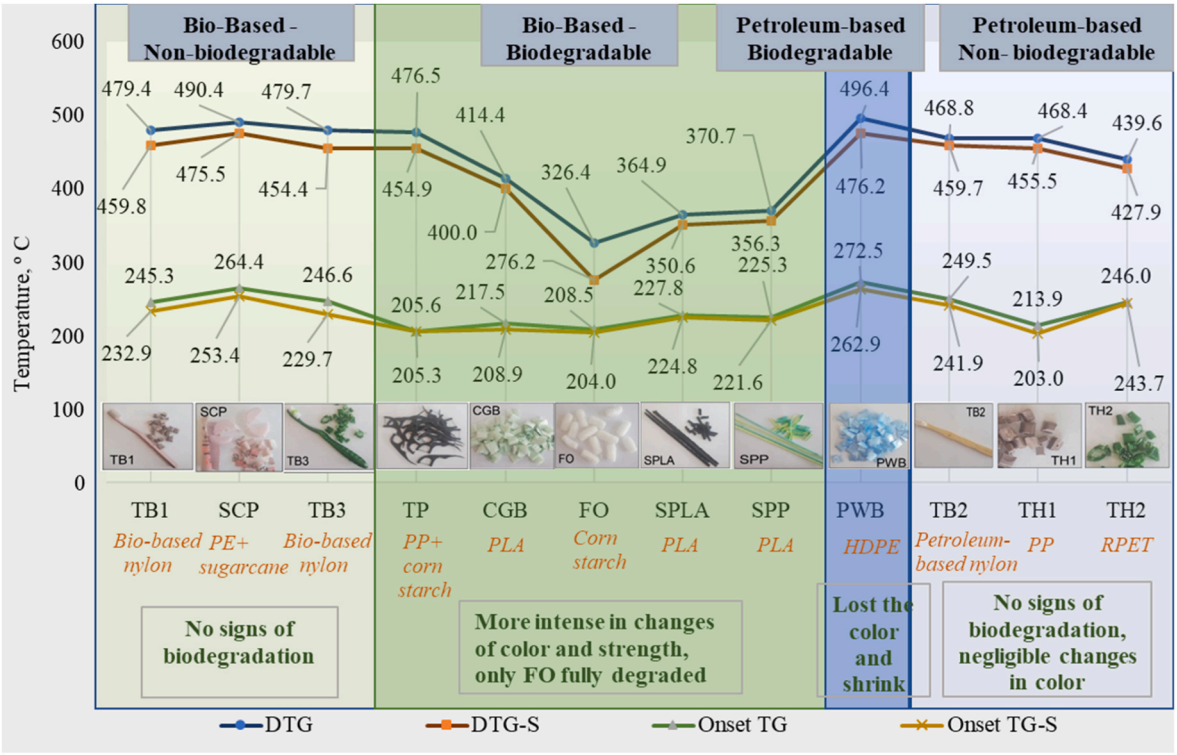

Fig. 9. Thermal degradation onsets and peaks of samples determined in nitrogen and steam environments.

TP, while FO, CGB, SPLA and SPP have decomposed in multiple stages. The multi-stage thermal decomposition is also supported by the result of multiple peaks in DTG curves. Thus, according to the obtained TGA-DTG curves, among all analysed plastic materials bioplastics assigned to the group B, specifically FO, CGB, SPLA and SPP are made of mixture of polymers with non-identical thermal decomposition temperatures (Fig. 8 A).

Comparing samples of group A, TB1 and TB3 had particularly close onset (Fig. 9: Onset TG, Onset TG-S) temperatures of thermal degradation that was equal to approximately 245.3 °C and 246.6 °C in the inert atmosphere along with 232.9 °C and 229.7 °C in the steam environment respectively. DTG (Fig. 9: DTG and DTG-S) peak temperatures were almost identical as well (respectively 479.6 °C and 457.1 °C) due to the fact that both plastics are made of nylon (Fig. 8 A, Fig. 9). In a previously conducted study of fresh nylon ropes by Pannase et al. [50] it was evaluated that nylon decomposes at the temperature range of 420–550 °C under heating rate of 5–10 °C/min during pyrolysis. Whereas, Sustaita-Rodríguez et al. [51] determined that nylon heated at 1 °C/min starts to decompose at 250 °C, as suggested by the results obtained in the present investigation. Meanwhile, third sample of group A (SCP) primarily made of PE has slightly higher thermal stability (Fig. 9) since it starts to degrade at ~264.4 °C with the highest mass loss rate at ~490.4 °C temperature during pyrolysis and at that of ~253.4 °C and ~475.5 °C during steam pyrolysis respectively. Similar results were obtained by Das and Tiwari [52] who have analysed the PE and PP packaging waste conversion by means of slow pyrolysis (heating rate – 1 °C/min) and had estimated that the PE begins to decompose between 330 and 340 °C with the highest decomposition rate observed at 430–435 °C temperature. The notable difference in decomposition onset temperature determined in the present and mentioned research may have occurred not only due to the differences in experimental conditions but also due to the semi-natural origin of the SCP sample, which has influenced thermal degradation of the sample at a lower temperature.

TGA-DTG graphs of bioplastics from the group B (Fig. 8 B) show that these samples have lower temperatures of thermal decomposition compared with the samples attributed to the rest groups (Fig. 8 C–D). The lowest temperatures of DTG peaks (Fig. 9) were determined to be of those plastics that were made of completely natural origin materials, that were FO, SPLA and SPP equal to 326.4 °C, 364.9 °C, 370.7 °C in nitrogen atmosphere and 276.2 °C, 350.6 °C, 356.3 °C temperature in steam atmosphere, respectively. Whereas the lowest thermal stability at both thermal decomposition environments was typical for TP sample (Fig. 9) made of PP and starch – the decomposition onset was determined at around 205.3–205.6 °C temperature. This may have been a consequence of corn starch presence in the composition of this plastic, whose degradation onset temperature is usually lower [53]. Previously carried out investigations of plastic wastes [52] have confirmed that PP begins to decompose at around 275 °C temperature. Additionally, it is concluded that TP sample is mostly made of PP and only a minor part of starch because only one decomposition stage was identified in TGA curve of the present sample. Contrarily, Roy et al. [54] investigated the physical-mechanical and thermal properties of the polypropylene and potato starch bio-composites and determined that such composites degrade in distinct stages visible in TGA curves starting from 280 °C. In terms of bioplastic sample FO, which is made of starch, had a particularly close degradation onset temperature (see Fig. 9) compared with TP, however FO sample underwent two weight loss stages caused by temperature elevation that were determined in TGA (Fig. 8). The second stage starting from around 350 °C was attributed to the carbonisation process of the sample. Corresponding results were obtained by Abbes et al. [54] who elaborated and characterised beet pulp and potato starch packaging foams. Another corn starch-derived sample – CGB, similarly to FO underwent couple events during thermal processing. The CGB sample (Fig. 9) started to degrade at 217.5 °C and 208.9 °C temperature in the N_2 atmosphere and steam pyrolysis respectively, with the main decomposition peaks estimated in DTG curves at 414.4 °C and 400 °C. While bioplastics made of polylactic acid (PLA) were determined to be more stable than starch-based bioplastic samples – SPLA and SPP (Fig. 9) thermal decomposition started at 227.8 and 225.3 °C during pyrolysis with N_2 and 224.8 and 221.6 °C respectively, when reactive atmosphere of steam was used. The highest mass loss rates were estimated to occur at 364.9–370.7 °C and 350.6–356.3 °C temperatures in N_2 and steam

atmosphere accordingly. The obtained results correspond to the investigation of PLA filaments for the 3D printing [55] which revealed that the main thermal degradation of this polymer occurs at 374 °C temperature, which is much lower compared to that of analysed petroleum-based plastics. Therefore, according to the TGA-DTG results of bioplastic samples attributed to the group B, the lower thermal stability was confirmed to be one of the characteristics of bio-based, biodegradable plastic materials.

The most thermally stable sample was determined to be the one assigned to the group C of plastics – PWB, made of high-density polyethylene (HDPE) with a Reverte additive (specific form of calcium carbonate) that assists in faster degradation of polymer in natural environment (Fig. 8 C). The decomposition onset of PWB (Fig. 9) was observed at 272.5 °C and 262.9 °C temperature in the inert and steam atmosphere, respectively. The sample also had the highest observed thermal degradation temperature determined from DTG curve that was 496.4 °C and 476.2 °C temperature in nitrogen and steam environment, respectively. Aigbodion et al. [56] conducted an analysis of HDPE pellets thermal stability and, similarly to the results obtained in this research, concluded that the main thermal decomposition of HDPE occurs at 487.5 °C when temperature is elevated at 20 °C/min rate in N_2 atmosphere. Thus, the conclusion is reached that Reverte additive has no significant effect on HDPE thermal stability and according to the TGA-DTG curves, the most thermally stable sample among all analysed plastics is PWB sample that is made of conventional HDPE.

High thermal stability was one of the properties of the plastic wastes classified in group D as well (Fig. 8 D). The highest onset temperature (Fig. 9) of degradation among plastics in the present group was determined to have TB2 sample primarily made of petroleum-derived nylon – 249.5 °C during pyrolysis and 241.9 °C in steam environment. Whereas, the greatest decomposition rate of TB2 sample was achieved at 468.8 °C and 459.7 °C temperature, respectively. Particularly close result was obtained with the bioplastic materials made of bio-based nylon of the group A. TH2 sample composed of 100% recycled PP exhibited analogous degradation temperatures to ones of TP sample attributed to the group B that was mostly made of non-recycled PP. In terms of the polyethylene terephthalate (PET) sample namely TH2 that was a 100% recycled polymer was observed to degrade at notably close temperature to one determined of TB2 sample of the present group of plastics. TH2 decomposition onset (Fig. 9) was estimated at 246 °C in the inert atmosphere and at 243.7 °C in steam ambient with the greatest mass loss rate at 439.6 °C and 427.9 °C respectively. Dhahak et al. [57] conducted a slow pyrolysis (2–30 °C/min) investigation of unused PET powder and concluded that the main decomposition temperature of this polymer is 421 ± 1 °C, which is a close result to the one determined in this research. It can be stated that the thermogravimetric analysis of bioplastics and conventional plastics have revealed that the origin of polymer has no significant effect on the thermal stability as long as it has matching chemical structure.

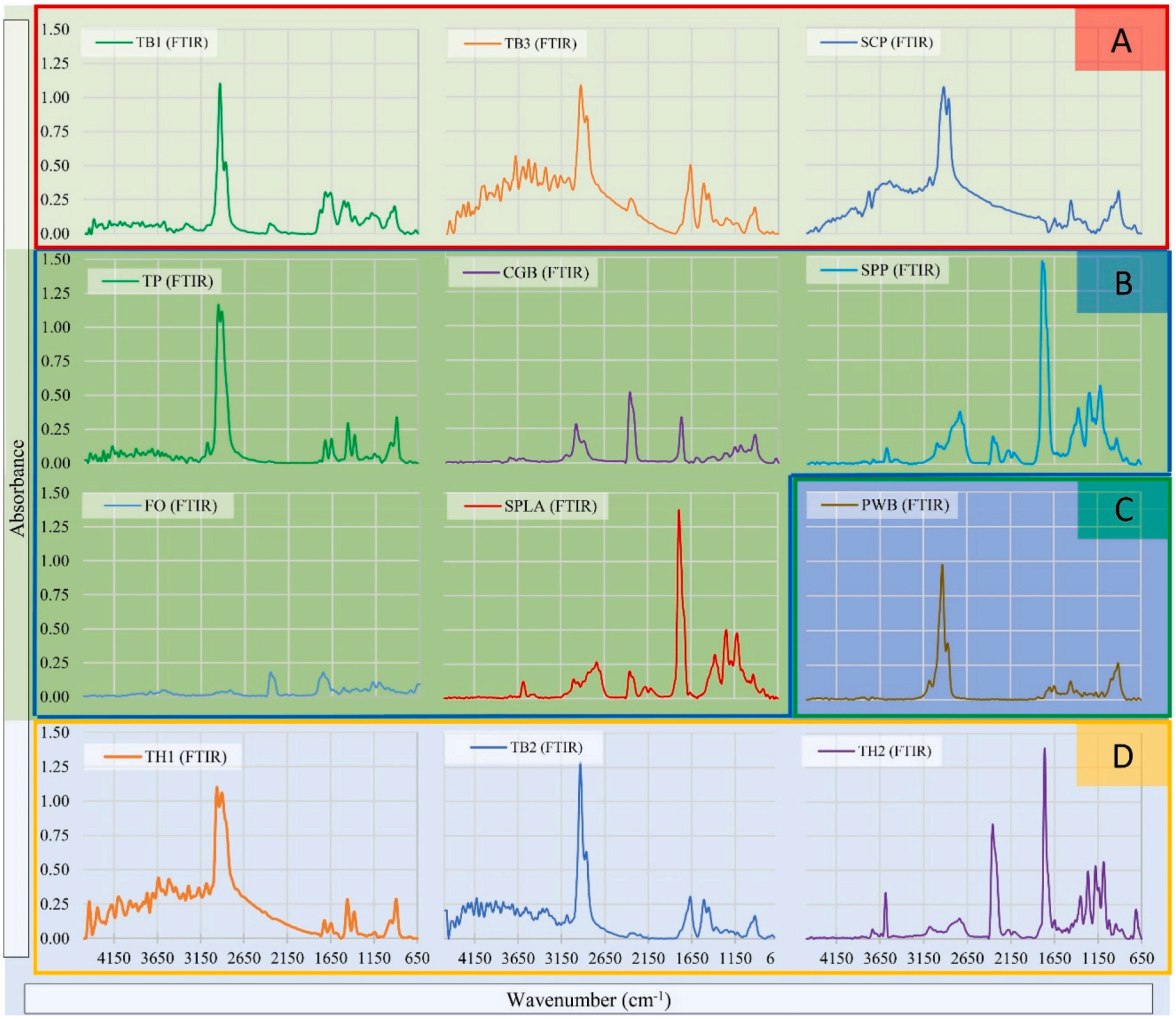

Fig. 10. IR absorption spectrums of volatile products formed during pyrolysis of selected bioplastic and plastic waste obtained by means of TG-FTIR approach.

3.3. Py-FTIR analysis

To evaluate the main groups and certain species of compounds evolved during the pyrolysis of plastic waste, FTIR analysis of gas stream was performed simultaneously. The FTIR measurements were carried out during full temperature range set in the TGA program and the absorption of IR reached the highest intensities at the main decomposition temperature (temperature of the DTG peak; see Fig. 9) of each sample. Therefore, absorbance graphs were extracted and analysed at exactly this specific degradation temperature of each analysed plastic material. Spectrums obtained during the analysis were grouped in accordance to the origin and degradability aspects of plastics. The IR absorbance spectrums of pyrolysis volatile products of four groups of plastics (A, B, C and D) are presented in Fig. 8.

It was determined that the first group of all plastics (Fig. 10 A) consisting of non-biodegradable bioplastics TB1, TB3 and SCP have similar thermal degradation properties in terms of composition of released gases. The main compounds evolved in these cases in accordance to the intensity of IR absorption were attributed to the aliphatic saturated species (one of the examples – methane), as well as solitary alkyl groups, since the highest absorbance at approximately 2925 cm^{-1} wavenumber was registered; that corresponds to the valence vibrations in C–H bonds. Some alkenes have formed as well, because these compounds tend to show absorbance of IR radiation in the close region to the referred one which is also proved by peaks at ~910 cm^{-1}. All three materials of the first group of analysed plastics tended to exhibit previously described absorption peaks, therefore these were the major similarities comparing pyrolysis products of TB1, TB3 and SCP samples. TB1 and TB3 are made of nylon (that has amino groups in the monomer of 1,6-diaminohexane) of natural origin, thus the formation of amines also took place during the pyrolysis of mentioned samples. It was proved by origination of IR absorption peaks at around 1650 cm^{-1} and 1500 cm^{-1} that correspond to the vibrations in N–H bonds. Since SCP is made from bio-bases PE and conventional PE, the formation of amines was not observed. Release of a small amount of CO_2 gas was also observedduring the thermal decomposition of TB1 and TB2 samples due to the presence of short absorption peaks at around 2340 cm^{-1}. Previously conducted research on nylon pyrolysis volatile products has also revealed equivalent results. Pannase et al. [50] analysed pyrolysis products of fresh nylon ropes by utilizing TG-FTIR approach and indicated that the main compounds in volatile fraction include alkanes, alkenes, amines and CO_2 that were detected in TG-FTIR spectrums of nylon samples in this research as well. In terms of distribution of PE pyrolysis products, Wu et al. [58] carried out a TG-FTIR research on pure PE resin and noted that the main groups of compounds evolved during pyrolysis process were the same as determined in this research – alkanes, olefins and some mono-aromatics. In our case, the formation of phenyl derivatives from SCP sample was also likely due to the small IR absorbance band beyond 3000 cm^{-1} as a consequence of the aromatisation process occurring during pyrolysis [59].

Other group of biodegradable samples characterized by natural or partially natural origin plastics have shown quite different trends in the formation of volatile products during pyrolysis. Comparing TG-FTIR spectrums of the second group (Fig. 10 B) of analysed plastic materials it was determined that bioplastics made of fully natural sources, namely CGB, FO, SPLA and SPP, tended to decompose into volatile products of similar or identical origin, only differences in extent of IR absorption were noted. However, one sample attributed to this group decomposed quite uniquely compared with the rest of the samples, according to the TG-FTIR spectrums obtained. It was assessed that TP plastic sample (made of 70% of corn starch bioplastic and of 30% of conventional propylene – PP) was more similar to the polymers of petroleum origin (C and D groups) along with bioplastics made of nylon in terms of distribution of pyrolysis volatile products. It was determined that the main thermal decomposition products of TP were aliphatic hydrocarbons such as alkanes and alkenes due to the largest IR absorption peak at wavenumber of 2952 cm^{-1} as well as minor peaks at 1454 cm^{-1}. The formation of aromatic species was also noted since the absorption of IR atapprox. 3071 cm^{-1} wavenumber that indicates C–H stretching which was confirmed by the absorption band at 1650 cm^{-1} that indicates C═C stretching in a benzene ring. In addition, absorption of IR rays at 894 cm^{-1} reveals mono-aromatic species as one of the products that have evolved during the pyrolysis of TP sample. The TG-FTIR spectrum of TP was seen to be more comparable with the PP waste TG-FTIR spectrums of investigations previously carried out. For example, Singhet et al. [48] have performed TG-FTIR analysis of pyrolysis and co-pyrolysis volatile products of plastic wastes separated from MSW, one of which was PP and determined that the main groups of compounds formed during the pyrolysis of PP were alkanes, alkenes and aromatic species, as confirmed by our case – the highest absorption band was registered at wavenumber value of 2965 cm^{-1} and attributed to saturated hydrocarbons. In terms of biodegradable bioplastic samples of completely natural origin (CGB, FO, SPLA and SPP), it was assessed that alkanes, as one of the characteristic pyrolysis products, evolve as well, although absorption bands are much lower compared to the TP sample. According to the locations and intensities of IR absorption peaks in TG-FTIR spectrums, SPP and SPLA (both made of polylactic acid) tend to decompose during pyrolysis into exactly the same volatile products of which the main one was attributed to the chemical species of carboxylic acids. This was concluded referring to the highest IR absorption band at wavenumber of 1776 cm^{-1}, indicating the molecular stretch vibration in C═O link. The evolution of carboxylic compounds also verifies absorption band at 3586 cm^{-1}, which also suggests the formation of water. High IR absorption peaks were also observed at 1361 cm^{-1} that have been attributed to the formation of other oxygen-containing compounds: esters, formed during pyrolysis of SPP and SPLA samples. Evolution of CO And CO_2 gases was taking place as well, in accordance to IR absorption bands at wavenumber values of 2121 cm^{-1} and 2362 cm^{-1}, indicating molecular vibrations in C≡O and C═O bonds of inorganic molecules, respectively. Some aliphatic and aromatic hydrocarbons have also formed since the IR absorption peaks were present at the previously described specific wavenumber ranges in the TG-FTIR spectrums. Respective results were obtained in the TG-FTIR/GC-MS investigation of 3D-printed polylactic acid waste, conducted by Zhang et al. [60] in which it was also confirmed that the main volatiles formed include carboxylic compounds, CO, CO_2 and alkanes. The last two samples of the bioplastic materials of B group – CGB and FO primarily made of starch have decomposed during the pyrolysis into volatile products with a similar distribution. However, in these cases the formation of CO_2 was the most prevailing. Carboxylic acids were the second most abundant compounds evolved in pyrolysis of CGB and FO plastics. The third most abundant group of volatile compounds formed during the decomposition in the inert atmosphere of these samples according to the IR absorption intensities were saturated hydrocarbons. A small amount of water evolved during the pyrolysis of CGB and FO samples as well, due to the IR absorption at ~3570 cm^{-1} wavenumber value caused by vibrations in the O–H bonds. Zong et al. [53] have carried out a TG-FTIR investigation of the main biomass components by performing pyrolysis and have detected that the main volatiles that form during starch pyrolysis are oxygen-containing compounds such as carboxylic and heterocyclic compounds. These results obtained with the plastic samples of natural origin are explained by the generally high oxygen content in the raw materials of which bioplastics were made, therefore the formation of carboxylic compounds and small molecules containing oxygen was a major event during pyrolysis of such materials.

A single plastic sample – PWB, made of HDPE (petroleum origin with Reverte additive) – was attributed to the third group of plastics analysed (Fig. 10 C). Present sample was unique compared with the other analysed petroleum-based polymers, since the included additive causes an oxy-biodegradability of such plastic product, making it biodegradable. Still, compared to the other samples, PWB tended to decompose into the same volatile compounds as nylon, as well as PP based samples during

pyrolysis. The main compounds evolved, as suggested by IR absorption intensity, were alkanes. Other characteristic compounds were olefins and aromatic compounds. Singh et al. [48] noted that the main volatile products formed during the pyrolysis of HDPE (separated from municipal waste) were identical to those determined in this investigation – saturated hydrocarbons of which the major one was methane, as well as alkenes and aromatic hydrocarbons. Thus, it was identified that Reverte additive had no significant impact on the distribution of pyrolysis volatile products of HDPE plastics.

TG-FTIR analysis of the fourth group of plastics (Fig. 10 D) to which petroleum based, non-biodegradable plastics were attributed, have revealed that FTIR spectrums obtained during pyrolysis of two samples, namely TH1 and TB2, are comparable, whereas the third plastic – TH2, included into this group, decomposes into volatile products of quite divergent distribution. It was determined that the main volatile products formed during the pyrolysis of recycled PP sample – TH1, equally to the sample from the B group of plastics – TP that is partially made of conventional PP – were primarily alkanes, along with alkenes and aromatic species to a lesser extent. Whereas, the TB2 sample made of petroleum-derived nylon decomposed into the same volatile products as the plastic samples made of bio-based nylon (TB1 & TB3) – the main compounds were alkanes, while aromatic hydrocarbons, alkenes, amines and CO_2 have been observed in a lesser content. Carbon dioxide evolution occurred due to the natural presence of carboxylic groups in the nylon polymer that are the main source of present gas during pyrolysis [61]. Since TH2 sample is primarily made of recycled polyethylene terephthalate (PET) that has two ester groups per each monomer unit – the formation of CO_2 gas was notable. This was determined by high IR absorbance peak at wavenumber value of 2358 cm^{-1} at the TG-FTIR spectrum. Although, the highest absorbance band was observed at 1760 cm^{-1}, by which carboxylic acids are identified.

It was also evaluated that other volatile pyrolysis products of TH2 sample were water, alcohols, aromatic and saturated hydrocarbons, CO gas and esters that were detected in accordance to the IR absorbance bands at 3733 cm^{-1}, 3581 cm^{-1}, 3075 cm^{-1}, 2732 cm^{-1}, 2150 cm^{-1} and 1351 cm^{-1} wavenumber values, respectively. Relevant research [48] has also concluded that the main volatile compounds formed during pyrolysis of PET wastes are oxygen-containing carboxylic compounds and evolution of hydrocarbons is less significant, which is explained by the high oxygen content in the PET polymer itself.

It could be noted that surrounding environment and ambient conditions need to be assessed in order to substitute conventional plastics with bioplastics. Even though this research covers a small number of available bioplastics from the hygiene and beauty industry, it lays grounds for further studies of bioplastics to assess their longevity or biodegradability, as it is essential to predict their utilization potential for cleaner environment. Considering that the main pyrolysis products of the analysed bioplastics are carboxylic compounds, alkanes, alkenes, aromatic hydrocarbons, amines, CO and CO_2, this provides an opportunity to sustainably reuse bioplastics for energy production. However, the biodegradable group is still a major concern, the bioplastics selected in this study did not degrade or degradation is under detection limits due to minimal change in the polymer chains (except for the sample made from natural corn starch) during a short degradation period. Therefore, further research is foreseen to focus on behaviour of biodegradable samples under varying anaerobic decomposition conditions and analysis of formed digestate.

4. Conclusions

The objective of this study was to investigate degradation in soil and characterize raw and treated bioplastics by FTIR-ATR and FTIR-TGA methods and to determine pyrolysis characteristics by TGA-FTIR methods providing an overview of the bioplastic waste. Based on the obtained results, the following conclusions can be drawn:

- Biodegradability test revealed that only the bioplastic made of corn starch fully degraded during short-term degradation in the soil, while other bio-based and petroleum-based plastics only changed the colour and became softer. Also, ATR-FTIR analysis has not indicated drastic changes in the structure during the 6-month period. In this context, it can be argued that plastics/bioplastics could be utilized using the same methods as used for conventional plastics.
- By means of TGA-DTG analysis it was determined that the degradation of bioplastics begins at 203.0–272.5 °C (Fig. 9). It could be concluded that investigated bio-based and biodegradable bioplastics have high thermal stability and the petroleum-based plastic made of high-density polyethylene with an inorganic Reverte additive has the highest thermal stability – the degradation starts at 272.5 °C. The environment reactivity influence on the temperature of degradation onset of analysed waste was also estimated. During performing of thermal analysis in the steam environment all samples had a tendency to decompose at approximately 10–20 °C lower temperature compared with the inert atmosphere which was a consequence of hydrolysis effect of the steam. This allows for energy saving conditions when waste is converted into higher value-added products.
- Py-FTIR analysis in this research has revealed that it is advantageous to convert bioplastics into combustible gases with yields between 80 and 99%. It was also confirmed that the main volatile products in all except one analysed group of plastics were aliphatic hydrocarbons only the bioplastics made of corn starch and polylactic acid decomposed primarily into carbonyl compounds and the formation of hydrocarbons was exclusively slight.
- The analysis of bioplastics and conventional plastics have revealed that the origin of polymer has no significant effect on the decomposition temperature, which means that the bioplastic should be managed under the same measures for energy recovery rather than biodegradation in landfills, as this could become additional source of microplastics due to the long duration of biodegradation.

Credit author statement

Raminta Skvorčinskienė: Supervision, Conceptualization, Investigation, Formal analysis, Writing - original draft preparation, Writing - review & editing. **Ieva Kiminaitė**: Investigation, Methodology, Writing - original draft preparation, Formal analysis, Writing - review & editing. **Lina Vorotinskienė**: Data Curation, Formal analysis, Writing - review & editing, Validation. **Adolfas Jančauskas**: Conceptualization, Investigation, Data Curation, Methodology, Writing - review & editing, Validation. **Rolandas Paulauskas**: Formal analysis, Writing - original draft preparation, Writing - review & editing, Validation.

Declaration of competing interest

The authors declare that they have no known competing financial interests or personal relationships that could have appeared to influence the work reported in this paper.

Data availability

Data will be made available on request.

References

[1] Moshood TD, Nawanir G, Mahmud F, Mohamad F, Ahmad MH, AbdulGhani A. Sustainability of biodegradable plastics: new problem or solution to solve the global plastic pollution? Curr Res Green Sustain Chem 2022;5:100273. https://doi.org/10.1016/j.crgsc.2022.100273.

[2] Brooks AL, Wang S, Jambeck JR. The Chinese import ban and its impact on global plastic waste trade. Sci Adv 2018;4. https://doi.org/10.1126/sciadv.aat0131.

[3] An analysis of European plastics production, demand and waste data. Plastics Europe association and European Association of Plastics Recycling and Recovery Organisations; 2021. https://plasticseurope.org/wp-content/uploads/2021/12/Plastics-the-Facts-2021-web-final.pdf.

[4] Tejaswini MSSR, Pathak P, Ramkrishna S, Ganesh PS. A comprehensive review on integrative approach for sustainable management of plastic waste and its associated externalities. Sci Total Environ 2022;825:153973. https://doi.org/10.1016/j.scitotenv.2022.153973.

[5] European Commission. A European strategy for plastics in a circular economy COM (2018) 28 final, brussels, Belgium, vol. 2018. Brussels: A European Strategy for Plastics in a Circular Economy; 2018. https://eur-lex.europa.eu/legal-content/EN/TXT/HTML/?uri=CELEX:52018DC0028&from=PT.

[6] Di Bartolo A, Infurna G, Dintcheva NT. A review of bioplastics and their adoption in the circular economy. Polymers 2021;13:1229. https://doi.org/10.3390/polym13081229.

[7] United Nations, Transforming our world: the 2030 agenda for sustainable development, (n.d.). https://sdgs.un.org/2030agenda.

[8] The circular economy and the bioeconomy—partners in sustainability copenhagen, vol. 2018. Denmark: European Environment Agency; 2018, ISBN 9789292139742.

[9] García-Depraect O, Bordel S, Lebrero R, Santos-Beneit F, Börner RA, Börner T, Muñoz R. Inspired by nature: microbial production, degradation and valorization of biodegradable bioplastics for life-cycle-engineered products. Biotechnol Adv 2021;53:107772. https://doi.org/10.1016/j.biotechadv.2021.107772.

[10] Van Roijen EC, Miller SA. A review of bioplastics at end-of-life: linking experimental biodegradation studies and life cycle impact assessments, Resources. Conserv Recycl 2022;181:106236. https://doi.org/10.1016/j.resconrec.2022.106236.

[11] Aslam M, Kalyar MA, Raza ZA. Polyvinyl alcohol: a review of research status and use of polyvinyl alcohol based nanocomposites. Polym Eng Sci 2018;58:2119–32. https://doi.org/10.1002/pen.24855.

[12] Lagaron JM, Lopez-Rubio A. Nanotechnology for bioplastics: opportunities, challenges and strategies. Trends Food Sci Technol 2011;22:611–7. https://doi.org/10.1016/j.tifs.2011.01.007.

[13] Siracusa V, Blanco I. Bio-polyethylene (Bio-PE), bio-polypropylene (Bio-PP) and bio-poly(ethylene terephthalate) (Bio-PET): recent developments in bio-based polymers analogous to petroleum-derived ones for packaging and engineering applications. Polymers 2020;12:1641. https://doi.org/10.3390/polym12081641.

[14] Rahman MH, Bhoi PR. An overview of non-biodegradable bioplastics. J Clean Prod 2021;294:126218. https://doi.org/10.1016/j.jclepro.2021.126218.

[15] Madhavan Nampoothiri K, Nair NR, John RP. An overview of the recent developments in polylactide (PLA) research. Bioresour Technol 2010;101:8493–501. https://doi.org/10.1016/j.biortech.2010.05.092.

[16] Chanprateep S. Current trends in biodegradable polyhydroxyalkanoates. J Biosci Bioeng 2010;110:621–32. https://doi.org/10.1016/j.jbiosc.2010.07.014.

[17] Jung H-W, Yang M-K, Su R-C. Purification, characterization, and gene cloning of an Aspergillus fumigatus polyhydroxybutyrate depolymerase used for degradation of polyhydroxybutyrate, polyethylene succinate, and polybutylene succinate. Polym Degrad Stabil 2018;154:186–94. https://doi.org/10.1016/j.polymdegradstab.2018.06.002.

[18] Xu K, Li Q, Xie L, Shi Z, Su G, Harper D, Tang Z, Zhou J, Du G, Wang S. Novel flexible, strong, thermal-stable, and high-barrier switchgrass-based lignin-containing cellulose nanofibrils/chitosan biocomposites for food packaging. Ind Crop Prod 2022;179:114661. https://doi.org/10.1016/j.indcrop.2022.114661.

[19] Steffan R, editor. Consequences of microbial interactions with hydrocarbons, oils, and lipids: biodegradation and bioremediation. Cham: Springer International Publishing; 2018. https://doi.org/10.1007/978-3-319-44535-9.

[20] Bioplastics market. European Bioplastics; 2020. accessed on 1 November 2020, https://www.european-bioplastics.org/market/.

[21] European-bioplastics, BIOPLASTICS facts and figures, (n.d.). https://www.european-bioplastics.org/news/publications/.

[22] Dang B-T, Bui X-T, Tran DPH, Hao Ngo H, Nghiem LD, Hoang T-K-D, Nguyen P-T, Nguyen HH, Vo T-K-Q, Lin C, Yi Andrew Lin K, Varjani S. Current application of algae derivatives for bioplastic production: a review. Bioresour Technol 2022;347:126698. https://doi.org/10.1016/j.biortech.2022.126698.

[23] Barboza LGA, Dick Vethaak A, Lavorante BRBO, Lundebye A-K, Guilhermino L. Marine microplastic debris: an emerging issue for food security, food safety and human health. Mar Pollut Bull 2018;133:336–48. https://doi.org/10.1016/j.marpolbul.2018.05.047.

[24] Nandakumar A, Chuah J-A, Sudesh K. Bioplastics: a boon or bane? Renew Sustain Energy Rev 2021;147:111237. https://doi.org/10.1016/j.rser.2021.111237.

[25] Li D, Lei S, Rajput G, Zhong L, Ma W, Chen G. Study on the co-pyrolysis of waste tires and plastics. Energy 2021;226:120381. https://doi.org/10.1016/j.energy.2021.120381.

[26] Surendran U, Jayakumar M, Raja P, Gopinath G, Chellam PV. Microplastics in terrestrial ecosystem: sources and migration in soil environment. Chemosphere 2023;318:137946. https://doi.org/10.1016/j.chemosphere.2023.137946.

[27] Xie W, Su J, Zhang X, Li T, Wang C, Yuan X, Wang K. Investigating kinetic behavior and reaction mechanism on autothermal pyrolysis of polyethylene plastic. Energy 2023;269:126817. https://doi.org/10.1016/j.energy.2023.126817.

[28] Feng S, Zhang P, Jiang P, Zhang Z, Deng J, Cao Z. Synthesis and application of high-stability bio-based plasticizer derived from ricinoleic acid. Eur Polym J 2022;169:111125. https://doi.org/10.1016/j.eurpolymj.2022.111125.

[29] Kai X, Yang T, Shen S, Li R. TG-FTIR-MS study of synergistic effects during co-pyrolysis of corn stalk and high-density polyethylene (HDPE). Energy Convers Manag 2019;181:202–13. https://doi.org/10.1016/j.enconman.2018.11.065.

[30] ISO_15512. Plastics — determination of water content. n.d, https://www.iso.org/standard/73834.html; 2019.

[31] ISO_21656:2021. Determination of calorific value. 60, n.d, https://www.iso.org/standard/71321.html; 2021.

[32] ISO_21656:2021. Solid recovered fuels — determination of ash content. 13., n.d, https://www.iso.org/standard/71321.html; 2021.

[33] ISO_22167:2021. Solid recovered fuels — determination of content of volatile matter. 15., n.d, https://www.iso.org/standard/72716.html; 2021.

[34] ISO_21663:2020. Solid recovered fuels — methods for the determination of carbon (C), hydrogen (H), nitrogen (N) and sulphur (S) by the instrumental method. n.d. Solid recovered fuels — Methods for the determination of carbon (C), hydrogen (H), nitrogen (N) and sulphur (S) by the instrumental method, (2020), https://www.iso.org/standard/71332.html; 2020.

[35] Kale G, Auras R, Singh SP, Narayan R. Biodegradability of polylactide bottles in real and simulated composting conditions. Polym Test 2007;26:1049–61. https://doi.org/10.1016/j.polymertesting.2007.07.006.

[36] Portarapillo M, Danzi E, Guida G, Luciani G, Marmo L, Sanchirico R, Di Benedetto A. On the flammable behavior of non-traditional dusts: dimensionless numbers evaluation for nylon 6,6 short fibers. J Loss Prev Process Ind 2022;78:104815. https://doi.org/10.1016/j.jlp.2022.104815.

[37] Xia Z, Kiratitanavit W, Facendola P, Yu S, Kumar J, Mosurkal R, Nagarajan R. A bio-derived char forming flame retardant additive for nylon 6 based on crosslinked tannic acid. Thermochim Acta 2020;693:178750. https://doi.org/10.1016/j.tca.2020.178750.

[38] Cervantes-Uc JM, Cauich-Rodríguez JV, Vázquez-Torres H, Garfias-Mesías LF, Paul DR. Thermal degradation of commercially available organoclays studied by TGA–FTIR. Thermochim Acta 2007;457:92–102. https://doi.org/10.1016/j.tca.2007.03.008.

[39] Jiang B, Ma Y, Wang L, Guo Z, Zhong X, Wu T, Liu Y, Wu H. Thermal decomposition mechanism investigation of hyperbranched polyglycerols by TGA-FTIR-GC/MS techniques and ReaxFF reactive molecular dynamics simulations. Biomass Bioenergy 2023;168:106675. https://doi.org/10.1016/j.biombioe.2022.106675.

[40] Herrera-Kao WA, Loría-Bastarrachea MI, Pérez-Padilla Y, Cauich-Rodríguez JV, Vázquez-Torres H, Cervantes-Uc JM. Thermal degradation of poly(caprolactone), poly(lactic acid), and poly(hydroxybutyrate) studied by TGA/FTIR and other analytical techniques. Polym Bull 2018;75:4191–205. https://doi.org/10.1007/s00289-017-2260-3.

[41] Amato P, Muscetta M, Venezia V, Cocca M, Gentile G, Castaldo R, Marotta R, Vitiello G. Eco-sustainable design of humic acids-doped ZnO nanoparticles for UVA/light photocatalytic degradation of LLDPE and PLA plastics. J Environ Chem Eng 2023;11:109003. https://doi.org/10.1016/j.jece.2022.109003.

[42] Legodi MA, de Waal D, Potgieter JH, Potgieter SS. Rapid determination of CaCO3 in mixtures utilising FT—IR spectroscopy. Miner Eng 2001;14:1107–11. https://doi.org/10.1016/S0892-6875(01)00116-9.

[43] Nuriyah L, Saroja G, Rohmad J. The effect of calcium carbonate addition to mechanical properties of bioplastic made from cassava starch with glycerol as plasticizer. IOP Conf Ser Mater Sci Eng 2019;546:042030. https://doi.org/10.1088/1757-899X/546/4/042030.

[44] Ma Z, Chen D, Gu J, Bao B, Zhang Q. Determination of pyrolysis characteristics and kinetics of palm kernel shell using TGA–FTIR and model-free integral methods. Energy Convers Manag 2015;89:251–9. https://doi.org/10.1016/j.enconman.2014.09.074.

[45] Bocchini S, Frache A, Camino G, Claes M. Polyethylene thermal oxidative stabilisation in carbon nanotubes based nanocomposites. Eur Polym J 2007;43:3222–35. https://doi.org/10.1016/j.eurpolymj.2007.05.012.

[46] Özdemir T. Gamma irradiation degradation/modification of 5-ethylidene 2-norbornene (ENB)-based ethylene propylene diene rubber (EPDM) depending on ENB content of EPDM and type/content of peroxides used in vulcanization. Radiat Phys Chem 2008;77:787–93. https://doi.org/10.1016/j.radphyschem.2007.12.010.

[47] Karimpour-Motlagh N, Khonakdar HA, Jafari SH, Panahi-Sarmad M, Javadi A, Shojaei S, Goodarzi V. An experimental and theoretical mechanistic analysis of thermal degradation of polypropylene/polylactic acid/clay nanocomposites. Polym Adv Technol 2019;30:2695–706. https://doi.org/10.1002/pat.4699.

[48] Singh RK, Ruj B, Sadhukhan AK, Gupta P. A TG-FTIR investigation on the co-pyrolysis of the waste HDPE, PP, PS and PET under high heating conditions. J Energy Inst 2020;93:1020–35. https://doi.org/10.1016/j.joei.2019.09.003.

[49] Masuda T, Kushino T, Matsuda T, Mukai SR, Hashimoto K, Yoshida S. Chemical recycling of mixture of waste plastics using a new reactor system with stirred heat medium particles in steam atmosphere. Chem Eng J 2001;82:173–81. https://doi.org/10.1016/S1385-8947(00)00347-8.

[50] Pannase AM, Singh RK, Ruj B, Gupta P. Decomposition of polyamide via slow pyrolysis: effect of heating rate and operating temperature on product yield and composition. J Anal Appl Pyrol 2020;151:104886. https://doi.org/10.1016/j.jaap.2020.104886.

[51] Sustaita-Rodríguez JM, Medellín-Rodríguez FJ, Olvera-Mendez DC, Gimenez AJ, Luna-Barcenas G. Thermal stability and early degradation mechanisms of high-density polyethylene, polyamide 6 (nylon 6), and polyethylene terephthalate. Polym Eng Sci 2019;59:2016–23. https://doi.org/10.1002/pen.25201.

[52] Das P, Tiwari P. The effect of slow pyrolysis on the conversion of packaging waste plastics (PE and PP) into fuel. Waste Manag 2018;79:615–24. https://doi.org/10.1016/j.wasman.2018.08.021.

[53] Zong P, Jiang Y, Tian Y, Li J, Yuan M, Ji Y, Chen M, Li D, Qiao Y. Pyrolysis behavior and product distributions of biomass six group components: starch, cellulose, hemicellulose, lignin, protein and oil. Energy Convers Manag 2020;216:112777. https://doi.org/10.1016/j.enconman.2020.112777.

[54] Roy SB, Ramaraj B, , S.C. Shit, Nayak SK. Polypropylene and potato starch biocomposites: physicomechanical and thermal properties. J Appl Polym Sci 2011;120:3078–86. https://doi.org/10.1002/app.33486.

[55] Wojtyła S, Klama P, Baran T. Is 3D printing safe? Analysis of the thermal treatment of thermoplastics: ABS, PLA, PET, and nylon. J Occup Environ Hyg 2017;14:D80–5. https://doi.org/10.1080/15459624.2017.1285489.
[56] Aigbodion VS, Hassan SB, Atuanya CU, Neife SI. Kinetics of Isothermal Degradation studies by Thermogravimetric Data: effect of orange peels ash on thermal properties of High density polyethylene (HDPE). J Mater Environ Sci 2012;3:1027–36.
[57] Dhahak A, Hild G, Rouaud M, Mauviel G, Burkle-Vitzthum V. Slow pyrolysis of polyethylene terephthalate: online monitoring of gas production and quantitative analysis of waxy products. J Anal Appl Pyrol 2019;142:104664. https://doi.org/10.1016/j.jaap.2019.104664.
[58] Wu J, Chen T, Luo X, Han D, Wang Z, Wu J. TG/FTIR analysis on co-pyrolysis behavior of PE, PVC and PS. Waste Manag 2014;34:676–82. https://doi.org/10.1016/j.wasman.2013.12.005.
[59] Williams PT, Taylor DT. Aromatization of tyre pyrolysis oil to yield polycyclic aromatic hydrocarbons. Fuel 1993;72:1469–74. https://doi.org/10.1016/0016-2361(93)90002-J.
[60] Zhang F, Sun Y, Li J, Su H, Zhu Z, Yan B, Cheng Z, Chen G. Pyrolysis of 3D printed polylactic acid waste: a kinetic study via TG-FTIR/GC-MS analysis. J Anal Appl Pyrol 2022;166:105631. https://doi.org/10.1016/j.jaap.2022.105631.
[61] He X, Zhu H, Huo Y, Wang W. Study on the formation mechanism of the pyrolysis products of lignite at different temperatures based on ReaxFF-MD. ACS Omega 2021;6:35572–83. https://doi.org/10.1021/acsomega.1c05275.